LJMU Research Online

Khazov, D, Yaron, O, Gal-Yam, A, Manulis, I, Rubin, A, Kulkarni, SR, Arcavi, I, Kasliwal, MM, Ofek, EO, Cao, Y, Perley, DA, Sollerman, J, Horesh, A, Sullivan, M, Filippenko, AV, Nugent, PE, Howell, DA, Cenko, SB, Silverman, JM, Ebeling, H, Taddia, F, Johansson, J, Laher, RR, Surace, J, Rebbapragada, UD, Wozniak, PR and Matheson, T

 Flash Spectroscopy: Emission Lines from the Ionized Circumstellar Material Around <10-Day-Old Type II Supernovae

http://researchonline.ljmu.ac.uk/id/eprint/5610/

Article

For more information please contact researchonline@ljmu.ac.uk

http://researchonline.ljmu.ac.uk/

FLASH SPECTROSCOPY: EMISSION LINES FROM THE IONIZED CIRCUMSTELLAR MATERIAL AROUND <10-DAY-OLD TYPE II SUPERNOVAE

D. Khazov[1], O. Yaron[1], A. Gal-Yam[1], I. Manulis[1], A. Rubin[1], S. R. Kulkarni[2], I. Arcavi[3,4], M. M. Kasliwal[2], E. O. Ofek[1],
Y. Cao[2], D. Perley[2], J. Sollerman[5], A. Horesh[1], M. Sullivan[6], A. V. Filippenko[7], P. E. Nugent[7,8], D. A. Howell[3,9],
S. B. Cenko[10], J. M. Silverman[11], H. Ebeling[12], F. Taddia[5], J. Johansson[5], R. R. Laher[13], J. Surace[13],
U. D. Rebbapragada[14], P. R. Wozniak[15], and T. Matheson[16]

[1] Benoziyo Center for Astrophysics, Faculty of Physics, The Weizmann Institute for Science, Rehovot 76100, Israel
[2] Astronomy Department, California Institute of Technology, 1200 E. California Boulevard, Pasadena, CA 91125, USA
[3] Las Cumbres Observatory Global Telescope Network, 6740 Cortona Drive, Suite 102, Goleta, CA 93111, USA
[4] Kavli Institute for Theoretical Physics, University of California, Santa Barbara, CA 93106, USA
[5] The Oskar Klein Centre, Department of Astronomy, Stockholm University, AlbaNova, SE-10691 Stockholm, Sweden
[6] School of Physics and Astronomy, University of Southampton, Southampton, SO17 1BJ, UK
[7] Department of Astronomy, University of California, Berkeley, CA 94720-3411, USA
[8] Computational Research Division, Lawrence Berkeley National Laboratory, 1 Cyclotron Road MS 50B-4206, Berkeley, CA 94720, USA
[9] Department of Physics, University of California, Santa Barbara, CA 93106, USA
[10] Astrophysics Science Division, NASA Goddard Space Flight Center, Mail Code 661, Greenbelt, MD 20771, USA
[11] Department of Astronomy, University of Texas at Austin, Austin, TX 78712, USA
[12] Institute for Astronomy, University of Hawaii, 2680 Woodlawn Drive, Honolulu, HI 96822, USA
[13] Spitzer Science Center, California Institute of Technology, M/S 314-6, Pasadena, CA 91125, USA
[14] Jet Propulsion Laboratory, California Institute of Technology, Pasadena, CA 91125, USA
[15] Los Alamos National Laboratory, Los Alamos, NM 87545, USA
[16] National Optical Astronomy Observatory, 950 North Cherry Avenue, Tucson, AZ 85719, USA

ABSTRACT

Supernovae (SNe) embedded in dense circumstellar material (CSM) may show prominent emission lines in their early-time spectra ($\leqslant$10 days after the explosion), owing to recombination of the CSM ionized by the shock-breakout flash. From such spectra ("flash spectroscopy"), we can measure various physical properties of the CSM, as well as the mass-loss rate of the progenitor during the year prior to its explosion. Searching through the Palomar Transient Factory (PTF and iPTF) SN spectroscopy databases from 2009 through 2014, we found 12 SNe II showing flash-ionized (FI) signatures in their first spectra. All are younger than 10 days. These events constitute 14% of all 84 SNe in our sample having a spectrum within 10 days from explosion, and 18% of SNe II observed at ages <5 days, thereby setting lower limits on the fraction of FI events. We classified as "blue/featureless" (BF) those events having a first spectrum that is similar to that of a blackbody, without any emission or absorption signatures. It is possible that some BF events had FI signatures at an earlier phase than observed, or that they lack dense CSM around the progenitor. Within 2 days after explosion, 8 out of 11 SNe in our sample are either BF events or show FI signatures. Interestingly, we found that 19 out of 21 SNe brighter than an absolute magnitude $M_R = -18.2$ belong to the FI or BF groups, and that all FI events peaked above $M_R = -17.6$ mag, significantly brighter than average SNe II.

Key words: supernovae: general

1. INTRODUCTION

Core collapse (CC) in massive stars ($M \gtrsim 8\,M_\odot$) results in various types of supernova (SN) explosions. Classification of such supernovae (SNe) is based primarily on their spectroscopic features (see, e.g., Filippenko 1997 for a review). In general, Type II SNe (SNe II) show prominent lines of hydrogen in their spectra, and SNe IIb also exhibit substantial He. Progenitors devoid of hydrogen result in SNe Ib that show helium lines, or SNe Ic that reveal neither hydrogen nor helium. SNe Ic having very broad lines in their spectra ($(2–3) \times 10^4 \, \mathrm{km \, s^{-1}}$) are classified as Type Ic-BL (and some of these are associated with gamma-ray bursts). Further classification among SNe II is based on their visual-wavelength light curves. SNe II-P show a plateau of ~100 days duration, while SNe II-L show a more linear (in magnitude) decay. The distinction between Types II-L and II-P is somewhat controversial (Arcavi et al. 2012; Anderson et al. 2014; Faran et al. 2014; Sanders et al. 2015).

Along their evolution and particularly during the post-main-sequence lifetime, massive stars tend to lose mass by either winds, binary interactions, or various eruptive events (e.g., Smith 2014). If the mass is lost from the progenitor shortly before it explodes as an SN, the interaction between the SN ejecta and the circumstellar material (CSM) may result in X-ray or radio emission for normal winds and in narrow optical emission lines for a dense CSM. The latter are classified as Type IIn (H lines; e.g., Schlegel 1990; Filippenko 1991; Kiewe et al. 2012; Taddia et al. 2013) or Type Ibn (He lines; e.g., Pastorello et al. 2008) SNe.

Intense mass loss via eruptive events sometimes manifests itself as precursors prior to the SN explosion (Ofek et al. 2014), as in SN 2006jc (Pastorello et al. 2007), SN 2010mc (Ofek et al. 2013), PTF11qcj (Corsi et al. 2014), and possibly SN 2009ip (whether an SN was finally produced is controversial; e.g., Mauerhan et al. 2013; Graham et al. 2014; Margutti et al. 2014; Ofek et al. 2014; Martin et al. 2015). Mass loss from

massive stars has an important role in their evolution and is critical in determining the type of the SN explosion. The physics and rates of mass loss are generally not well understood, and the rates used in stellar evolution models are quite uncertain (Langer 2012; Smith 2014).

Optical spectra obtained a short time (a few days or less) after an SN explosion may be dominated by features generated by ionization of the CSM by ultraviolet (UV) radiation emitted during the hot shock breakout and the early shock-cooling phase (SN 2013cu = iPTF13ast; Gal-Yam et al. 2014). The photons emitted from the SN ionize the material around the progenitor (if such exists), and this CSM recombines and radiates strong emission lines. It is possible that further emission is generated by collisional excitations by the free electrons. From a series of spectra showing these emission lines, we can learn about the elemental abundances in the CSM, the early temperature evolution of the ejecta, and the progenitor mass-loss rate shortly prior to the explosion (e.g., Groh 2014; Shivvers et al. 2015; Smith et al. 2015). We refer to the method of obtaining such early-time spectra as "flash spectroscopy" and the spectra showing such emission features as "flash ionized" (FI; Gal-Yam et al. 2014). Previous examples of early-time spectra that are FI were presented for SN 1983K (Niemela et al. 1985; Phillips et al. 1990), SN 1993J (Garnavich & Ann 1994; Matheson et al. 2000), SN 1998S (Leonard et al. 2000; Shivvers et al. 2015), and SN 2006bp (Quimby et al. 2007).

Following the detection of FI signatures in iPTF13ast (Gal-Yam et al. 2014), we have searched for additional similar events in the Palomar Transient Factory (PTF; Law et al. 2009; Rau et al. 2009) and intermediate PTF (iPTF) spectroscopic databases from 2009 through the end of 2014, showing prominent high-ionization (in particular, He II $\lambda4686$) emission lines in early-time spectra that later disappear. Our main motivation is to quantify the frequency of such objects and hence the fraction of progenitors embedded in CSM. We find that a substantial fraction of SNe show FI signatures in their early-time spectra, and the majority of SNe II observed a few days after explosion have spectra that either are blue and featureless or exhibit prominent emission lines.

In Section 2 we present the observations, the sample construction, and the SN classification criteria. Our results are given in Section 3. In Sections 4 and 5 we discuss and summarize the main ideas.

2. OBSERVATIONS AND SAMPLE CONSTRUCTION

The SN discoveries, classifications, and redshifts were obtained as part of the PTF and iPTF surveys. The SN discovery is confirmed by on-duty astronomers, who also trigger follow-up observations. A review of the real-time alert system and follow-up programs can be found in Gal-Yam et al. (2011), and the latest machine-learning procedures in use (distinguishing a real source from a bogus artifact) are described in Brink et al. (2013), Wozniak et al. (2013), and Rebbapragada et al. (2015). UT dates are used throughout this paper. All epochs are given in the observer's frame; the redshifts of the SNe in our sample are low ($z < 0.2$), and the corrections are negligible for our purposes. Table 1 summarizes the details of the SNe whose spectra are presented in this paper: the 12 FI SNe and the three events younger than 2 days that are neither FI nor blue/featureless (see Section 2.3).

2.1. Spectra

All spectra used for this work were obtained as part of the PTF survey and were available via our internal (Marshal) database. The details of the spectra are summarized in Table 2. These data are made public via the WISeREP portal (Yaron & Gal-Yam 2012). Spectral reductions were carried out using standard procedures. Full discussions of our spectroscopic data sets will be reported in future publications.

2.2. Photometry

PTF survey images are obtained by the survey camera (Rahmer et al. 2008) mounted on the Palomar 48-inch Schmidt telescope in the Mould R or Gunn g bands. Transient discovery is performed by an automated real-time pipeline using image subtraction (e.g., Gal-Yam et al. 2011). The system provides preliminary automated photometry,[17] which can often be improved. Full processing is then conducted using the PTF/IPAC pipeline (Laher et al. 2014), and the data are photometrically calibrated (Ofek et al. 2012).

In this paper, we present photometry that has been processed through our custom image-subtraction pipelines,[18] following the IPAC/PTF photometric pipeline. Our image-subtraction pipeline has been used extensively in earlier PTF science publications (e.g., Firth et al. 2015, and references therein). The co-add reference for each object was constructed from images taken up to 20 days before the discovery, using the same filter as when the object was detected by the automated pipeline. The pipeline subtracts the reference from every image, performs point-spread function (PSF) photometry on the result, and provides the calibrated flux and the flux uncertainty for each of the images, using the Sloan Digital Sky Survey (SDSS; when available) or PTF zero points. The detection threshold is set to be 3 times the 1σ flux uncertainty. All values have been converted to the native PTF photometric system (Ofek et al. 2012).

The photometry presented here is corrected for Galactic extinction by calculating E_{B-V} according to Schlegel et al. (1998) and the extinction following Cardelli et al. (1989). No K-corrections were applied, given the low redshifts of the SNe in our sample ($z < 0.2$).

2.3. Sample Construction and SN Classification

Our sample consists of 103 CC SNe, 84 of them of Type II (Figure 1(a)), discovered by the PTF and iPTF surveys between 2009 and 2014, whose first spectra were obtained within 10 days from the time of the SN pre-explosion limit. We chose the pre-explosion limit as the last nondetection where the limiting magnitude (the nondetection threshold) is fainter by 0.5 mag than the first detection. For SNe with a well-sampled rise to peak, we used a parabolic fit and estimated the explosion time and the pre-explosion limit as the time when the flux is 0. We decided to focus on SNe younger than 10 days after an initial inspection of the first spectra of SNe obtained within 6 days from the discovery. These events include a large population of old SNe (sometimes discovered a long time after their last nondetection), and we found that all of the events of interest (showing FI

_____

[17] This is internally referred to as the "Nugent pipeline."
[18] These are internally referred to as the "Sullivan pipeline" and PTFIDE.

Table 1
15 PTF and iPTF Supernovae with Early-time Spectroscopy

Name	α (degree)	δ (degree)	Spectroscopic Classification	Redshift	First Detection Date[a]	R Detection Mag	Latest Nondetection Limit Date[a]	Limiting Mag	Estimated Explosion Time	First Spectrum Date[a]	References
PTF09ij	218.061018	54.855424	SN II	0.124	2009 May 20.29 [2.01]	21.05	2009 May 16.28 [−2.01]	21.82	2009 May 18.28	2009 May 21.28 [3]	⋯
PTF10abyy	79.16885	6.798268	SN II	0.0297	2010 Dec 03.32 [0.51]	21.14	2010 Dec 02.31 [−0.51]	21.88	2010 Dec 02.82	2010 Dec 09.6 [6.79]	⋯
PTF10gva	185.98082	10.580728	SN II	0.0276	2010 May 05.17 [0.9]	18.13	2010 May 03.38 [−0.9]	21	2010 May 04.27	2010 May 06.4 [2.12]	⋯
PTF10gvf	168.438496	53.629126	SN IIn	0.081	2010 May 04.31 [0.65]	21.44	2010 May 03.66 [0]	N.A[b]	2010 May 03.66	2010 May 06.52 [2.86]	Ofek et al. (2014)
PTF10tel	260.377817	48.129834	SN IIn	0.035	2010 Aug 20.22 [2.5]	21.99	2010 Aug 17.72 [0]	N.A[b]	2010 Aug 17.72	2010 Aug 26.26 [8.53]	SN 2010mc; Ofek et al. (2013)
PTF10uls	20.344412	4.891319	SN II	0.0479	2010 Sep 07.43 [0.48]	21.21	2010 Sep 06.48 [−0.48]	21.78	2010 Sep 06.96	2010 Sep 10.44 [3.48]	Ofek et al. (2014)
PTF11iqb	8.52015	−9.704979	SN II	0.0125	2011 Jul 23.37 [1.1]	16.89	2011 Jul 22.27 [0]	N.A[b]	2011 Jul 22.27	2011 Jul 24.33 [2.06]	Smith et al. (2015); Ofek et al. (2014)
PTF12gnn	239.705326	36.169707	SN II	0.0308	2012 Jul 09.36 [0.97]	18.83	2012 Jul 07.43 [−0.97]	20.61	2012 Jul 08.39	2012 Jul 12.36 [3.97]	⋯
PTF12krf	342.069469	24.149513	SN II	0.0625	2012 Nov 04.13 [0.99]	20.65	2012 Nov 02.15 [−0.99]	21.27	2012 Nov 03.14	2012 Nov 07.19 [4.05]	⋯
iPTF13ast	218.495242	40.239672	SN IIb	0.0258	2013 May 03.18 [0.16]	20.22	2013 May 03.02 [0]	N.A[b]	2013 May 03.02	2013 May 03.5[c] [0.48]	SN 2013cu; Gal-Yam et al. (2014)
iPTF13dqy	349.936251	10.184555	SN II	0.011855	2013 Oct 06.25 [0.45]	18.63	2013 Oct 05.34 [−0.45]	20.71	2013 Oct 05.79	2013 Oct 06.38 [0.59]	O. Yaron et al. (2016, in preparation)
iPTF14bag	185.292993	64.343544	SN II	0.116	2014 May 18.23 [0.02]	20.64	2014 May 18.19 [−0.02]	21.37	2014 May 18.21	2014 May 21.34 [3.13]	⋯
iPTF13aaz	169.737245	13.063896	SN II-P	0.002692	2013 Mar 22.17 [1.42]	16.26	2013 Mar 19.34 [−1.42]	20.96	2013 Mar 20.75	2013 Mar 22.5 [1.74]	SN 2013am Zhang et al. (2014)
iPTF13dkk	355.396485	3.725103	SN II	0.0092	2013 Sep 12.19 [0.35]	18.91	2013 Sep 11.49 [−0.35]	21.39	2013 Sep 11.84	2013 Sep 12.99 [1.15]	⋯
iPTF14ayo	181.512516	47.492568	SN II	0.0023	2014 May 14.16 [0.49]	18.72	2014 May 13.19 [−0.49]	20.7	2014 May 13.68	2014 May 14.5 [0.82]	⋯

Notes.
[a] All dates are UT. In brackets: the time in days from the estimated explosion.
[b] We obtained the limit by fitting the rise time.
[c] This spectrum does not contain observed wavelengths below 4900 Å. We present a spectrum obtained a few days later.

Table 2
Log of Spectroscopic Observations

Name	UT Date	Telescope	Instrument	Observer	Reducer	He II λ4686 EW (Å)	Reference
PTF09ij	2009 May 21.28	Palomar 5.1 m	DBSP	Kasliwal	Kasliwal	-6.85 ± 0.48	⋯
PTF10abyy	2010 Dec 09.60	Keck I 10 m	LRIS	Ebeling	Cenko	-8.59 ± 0.15	⋯
PTF10gva	2010 May 06.39	Keck I 10 m	LRIS	Cenko et al.	Cenko	-2.65 ± 0.06	⋯
PTF10gvf	2010 May 06.52	Keck I 10 m	LRIS	Cenko et al.	Cenko	-4.83 ± 0.34	⋯
PTF10tel	2010 Aug 26.26	Gemini N 8 m	GMOS	Service	Howell, Murray	-2.93 ± 0.27	⋯
PTF10uls	2010 Sep 10.44	Kitt Peak 4 m	RC Spec	Kulkarni, Cenko	Cenko	-4.34 ± 0.36	⋯
PTF11iqb	2011 Jul 24.33	Gemini S 8 m	GMOS	Service	Parrent	-7.21 ± 0.18	⋯
PTF12gnn	2012 Jul 12.36	Lick 3 m	Kast	Clubb, Filippenko	Silverman	-3.37 ± 0.12	⋯
PTF12krf	2012 Nov 07.19	Palomar 5.1 m	DBSP	Horesh, Tang	Yaron	-2.74 ± 0.15	⋯
iPTF13ast	2013 May 06.01	Nordic Optical Tel.	ALFOSC	Geier (Service[a])	Taddia	-4.58 ± 0.13	⋯
iPTF13dqy	2013 Oct 06.38	Keck I 10 m	LRIS	Perley	Perley	-10.30 ± 0.22	⋯
iPTF14bag	2014 May 21.33	Apache Point 3.5 m	DIS	Cao	Cao	-8.74 ± 0.41	⋯
iPTF13aaz	2013 Mar 22.50	Lick 3 m	Kast	Fox et al.	Silverman	⋯	⋯
iPTF13dkk	2013 Sep 12.99	Nordic Optical Tel.	ALFOSC	Taddia, Van Eylen	Johansson	⋯	⋯
iPTF14ayo	2014 May 14.29	Gemini N 8 m	GMOS	Service	Cenko	⋯	⋯
SN 1993J	1993 Mar 30	Lick 3 m	Kast	Davis, Schlegel	⋯	-0.24 ± 0.05	Matheson et al. (2000)
SN 1998S	1998 Mar 04	Keck II 10 m	HIRES	Matheson, Filippenko	Shivvers	-10.50 ± 0.10	Shivvers et al. (2015)
SN 2006bp	2006 Apr 11	HET 9.2 m	LRS	Quimby	⋯	-1.00 ± 0.05	Quimby et al. (2007)

Note.
[a] ToO program, PI G. Leloudas.

signatures) were younger than 10 days from the time of the pre-explosion limit. For additional details see the Appendix.

For all of our events we use the improved photometry to estimate the explosion time, either using a parabolic fit as explained above, or as the mean between the times of the pre-explosion limit and the first detection.

We then classified all SNe based on their earliest spectra as either "blue/featureless" (BF), "flash ionized" (FI), or neither. A BF spectrum resembles the spectrum of a blackbody, without any prominent emission or absorption lines, and without broad P Cygni profiles (ignoring host-galaxy emission lines, night-sky lines, or any features caused by imperfect spectral reduction; Figure 2). The spectra of SNe classified as FI show a blue continuum with various emission lines, including in particular He II λ4686, accompanied by H Balmer lines, with widths corresponding to a velocity dispersion of $\sim1000\,\mathrm{km\,s}^{-1}$.[19] Since the H lines can be easily contaminated by narrow host-galaxy emission but the He II generally cannot, we focus on the He II λ4686 line. Moreover, its width corresponds to velocities much lower than those associated with the SN explosion, so its presence provides good evidence for emission from CSM ionized by UV radiation. We considered objects with persistent emission lines (SNe Ibn or IIn) as having flash-ionization signatures only if certain features (in particular, the He II line) disappeared in later spectra (Figure 2). We found that all events classified as FI or BF are

SNe II,[20] so from now on we focus our discussion on the 84 SNe II in our sample.

We quantify the level of He II λ4686 emission in spectra of the 84 objects included in our final sample by calculating the equivalent width (EW) of an emission line located in the range 4666–4706 Å. The continuum is fitted by a linear function in the range of 4545–4620 Å on one side and 4726–4800 Å on the other. In order to estimate the significance of any detection, we conduct the following simulation. We randomly choose a continuous subrange of at least 30% of our continuum area (yielding subranges with a mean of ~40 Å and a standard deviation of ~12 Å on each side) and recalculate the EW. By repeating this procedure 500 times, we estimate the uncertainty in the EW as the standard deviation of the results. We adopt as significant only cases where the relative error $\Delta \mathrm{EW}/\mathrm{EW} < 0.1$ (attributing any weaker detections to noise or to uncertain continuum estimation). We classify as FI events those having $\mathrm{EW} < 0$. We list the He II λ4686 EW values in FI spectra in Table 2. We also calculated the EW values of He II in the early-time spectra of previous events (except for SN 1983K, whose spectra are not available in electronic format), and they are presented as well in Table 2. These events would indeed be counted as FI events according to our selection criteria.

More details regarding the sample construction and the estimation of SN explosion times are given in the Appendix.

---

[19] The line is broadened by a combination of Doppler velocity and electron scattering which may be dominant (see, e.g., Groh 2014).

[20] We exclude a peculiar object of uncertain nature that possibly shows FI signatures and is the subject of a forthcoming publication (M. M. Kasliwal et al. 2016, in preparation).

(a) All Core-Collapse Supernovae

(b) Blue/Featureless Supernovae

(c) Flash-Ionized Supernovae
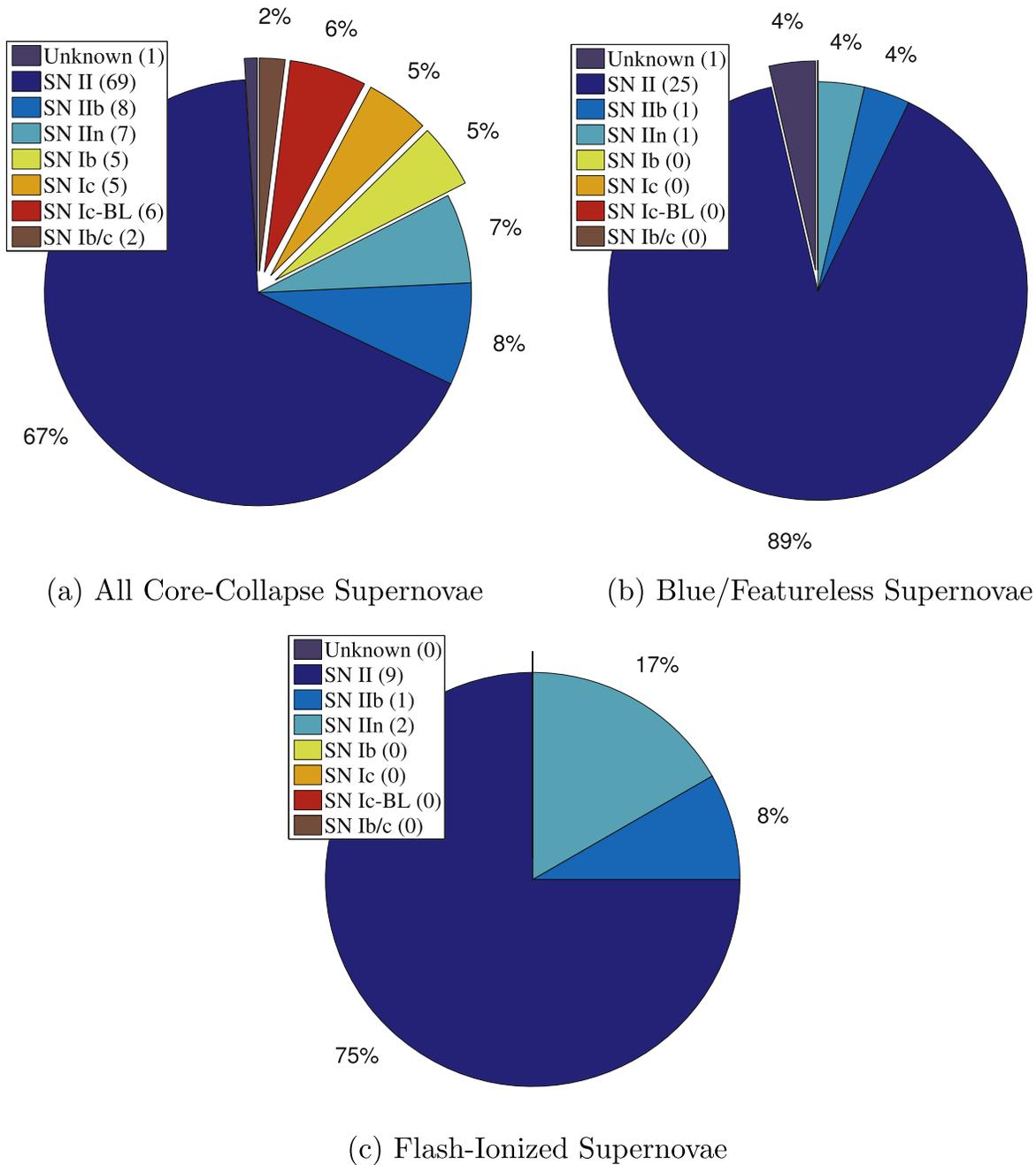
Figure 1. (a) Distribution by type of all 103 CC SNe whose first spectrum was taken <10 days after the time of the pre-explosion limit. Of these, 84 are SNe II. (b) Type distribution of events with BF first spectra (28 total). (c) Type distribution of FI SNe (12 total). There is only a single, featureless spectrum of the "unknown" SN, not enough for classification.

3. RESULTS

3.1. Spectral Classification

The distribution by type of the entire sample, the BF SNe, and the FI events is presented in Figure 1. Among the 12 FI events, one is of Type IIb, two are SNe IIn, and the rest are SNe II. The spectra of FI events are shown in Figure 3, and close-up views of the He II, Hα, and Hβ ranges are presented in Figure 4. The corresponding photometry is presented in Figure 5.

Within two days after the estimated explosion, we found three SNe that have neither FI signatures nor a blue continuum in their first spectra; see Figure 6. iPTF13aaz and iPTF13dkk have already developed broad lines <2 days after explosion.

iPTF14ayo is highly reddened, so its true spectroscopic nature is unclear. The photometry of two of the events can be found in Figure 5, while iPTF14ayo, owing to high reddening, has a very faint (> -12 mag) light curve that is omitted from the plot.

Well-observed FI events having a series of spectra taken a few days apart demonstrate that the SN FI signatures disappear over time, making the spectrum featureless, and subsequently P Cygni lines develop (Figure 2).

3.2. Fractions

A histogram showing the number of FI and BF events with respect to the age in days after explosion is presented in Figure 7. Event fractions are given in Table 3.
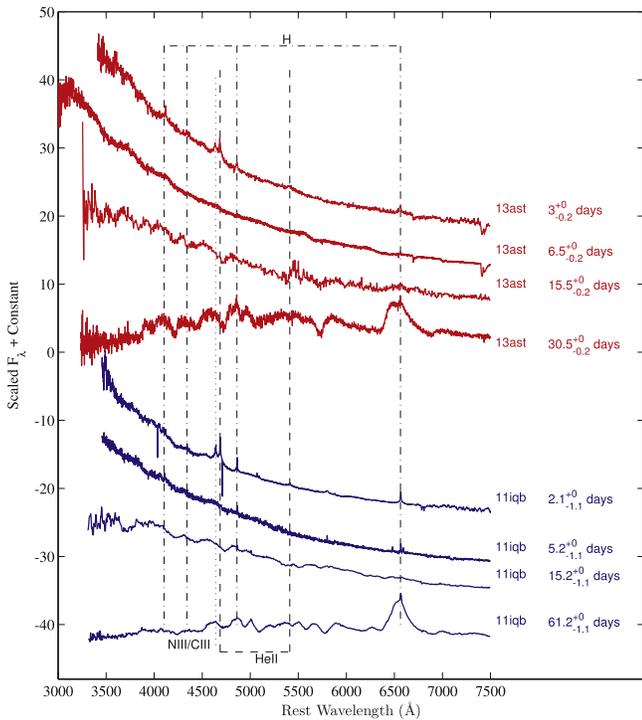
Figure 2. Spectral evolution of two of the FI events. The emission lines disappear within a few days, and P Cygni line profiles develop over time. These well-observed objects would be classified as FI if found prior to day 3 and as BF if found around day 5, demonstrating the evolution of SNe II, and why our measured FI fraction is only a lower limit on the true frequency of SNe having dense CSM. Data from Gal-Yam et al. (2014) and Smith et al. (2015).
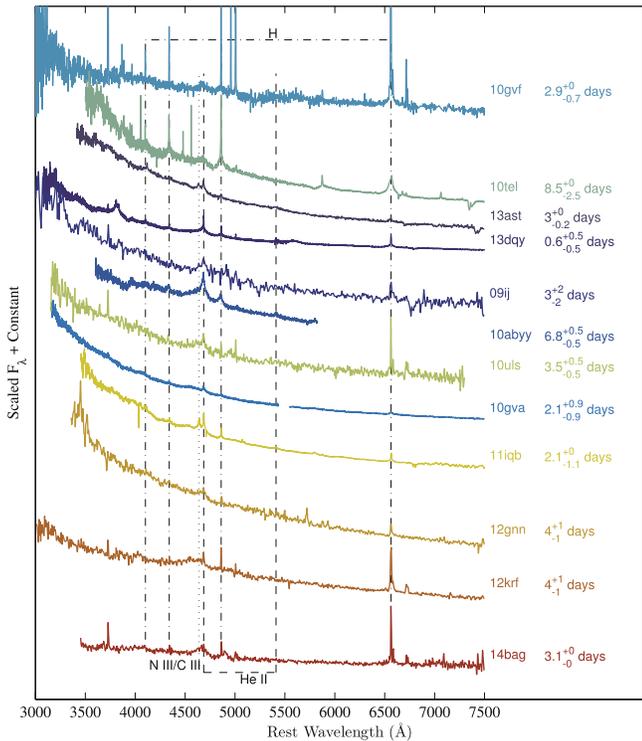
Figure 3. Spectra of our 12 FI events. On the right: an estimate of the age of the SN, with respect to the estimated explosion time (see the Appendix for details).

Assuming a binomial distribution where an event can be classified either as FI or not, the 68% confidence interval on the fraction of FI events given the available sample is in the range 7%–36%, 13%–24%, and 11%–19% within 2, 5, and 9 days after the explosion, respectively.

4. DISCUSSION

The FI fractions we found are significant (∼15%), yet these are clearly lower limits on the true fractions. The SNe that initially show FI signatures develop BF spectra at some later point (Figure 2). It is quite possible that the SNe showing a blue continuum in their first spectrum would have exhibited FI signatures at an earlier phase. Therefore, if we had earlier spectra of the entire sample, we would have observed a higher fraction of FI events. It is also possible that FI events were not detected owing to the low signal-to-noise ratio in some of the spectra. In addition, there is possible contamination by slowly rising old events that appear to be younger and satisfy our cut of the pre-explosion limit being only 0.5 mag deeper than the detection (see the Appendix for details). Future samples of events with systematic early-time spectroscopy should provide a more accurate estimate of the fraction of SN progenitors embedded in dense CSM. Our work demonstrates that this is not a rare occurrence.

An interesting result can be seen by inspecting Figure 8, which shows the natural connection between the redshift and the SN peak luminosity,[21] as expected in flux-limited surveys like PTF. SNe with FI signatures or a BF spectrum are more luminous on average than the other SNe in our sample. This is true even when we exclude the three SNe IIn that are classified as FI or BF. Using the Kolmogorov–Smirnov test, we reject the possibility that the peak-magnitude distribution of the FI and BF SNe is the same as that of the rest of the events, with a confidence level higher than 99.9%. Since SNe showing FI signatures or a BF continuum in their spectra are typically hotter (as hydrogen remains ionized and broad lines do not appear), we can conclude that more luminous SNe have higher temperatures at comparable ages than less luminous ones. It is unlikely that the high peak luminosity is caused by the interaction with the CSM (excluding SNe IIn), since the emission lines usually do not last for more than 10 days, while the events typically maintain their high luminosity for >20 days.

To estimate the fraction of FI and BF events in a volume-limited survey, we inspected all events at $z < 0.02$, where our survey is sensitive to SNe with a peak absolute magnitude $R < -14$ (Figure 8). Within the statistical uncertainty, we obtain the same fractions as for the entire sample. Our accuracy is limited by the small number of events at $z < 0.02$ (just 14). A larger sample may show lower fractions of FI and BF events in a volume-limited survey, since flux-limited data miss mostly the low-luminosity events that are usually neither FI nor BF.

Type II-P events are the most common among CC SNe (Smartt et al. 2009) and constitute almost 30% of CC SNe in an ideal magnitude-limited sample (Li et al. 2011, their Figure 11). Typically, SNe II-P display a plateau in their light curve for ∼100 days (Arcavi et al. 2012), with an absolute magnitude of $M_R \approx -16$. However, Figure 5 shows that none

---

[21] Luminosity as measured, not necessarily the peak of the true SN light curve.
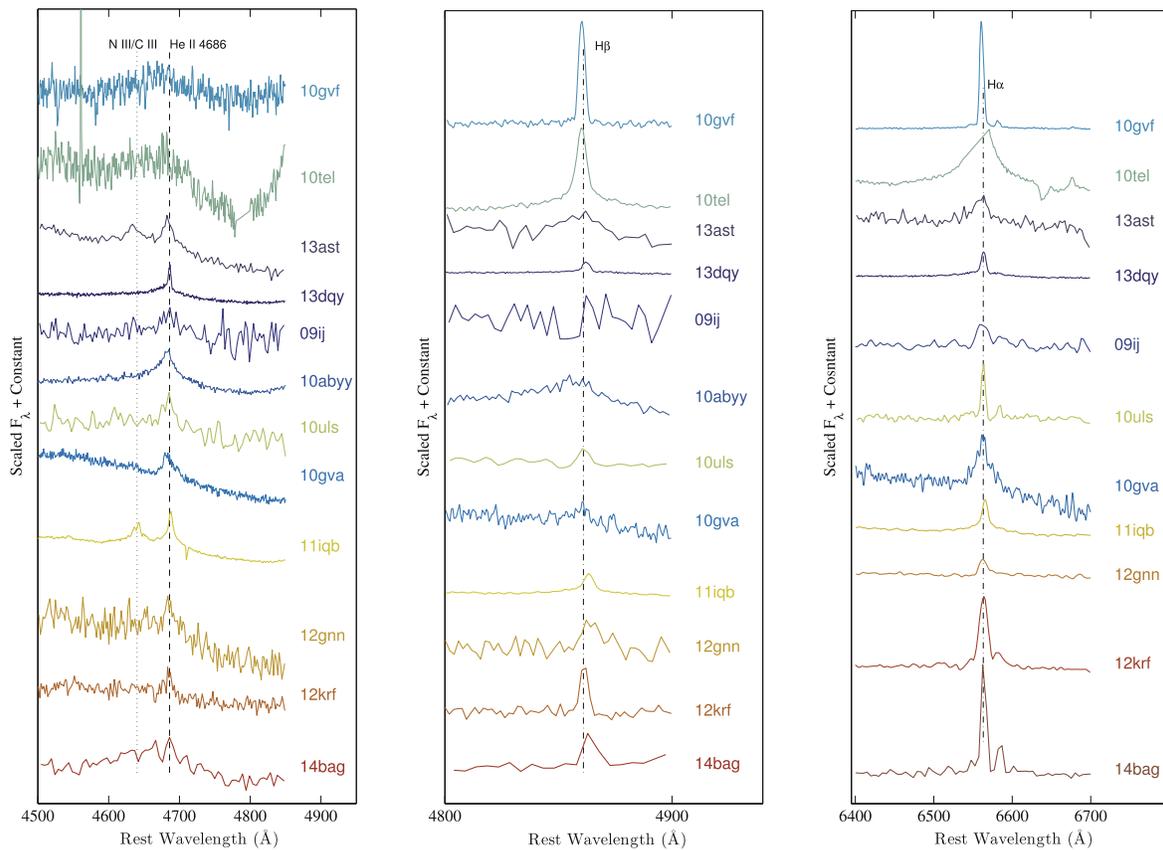
**Figure 4.** Close-up views of the Hα, Hβ, and He II regions in the first spectra of FI events.
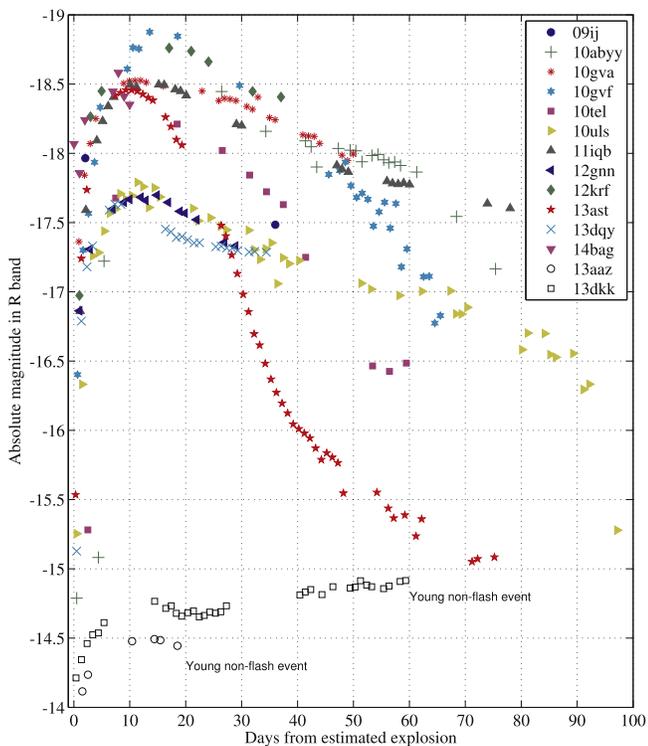
Figure 5. *R*-band photometry of the 12 flash-spectroscopy events and two (out of the three) events showing neither FI signatures nor a BF continuum in their spectra <2 days after explosion. The light curve of the highly reddened iPTF14ayo is very faint; it is omitted for clarity. Measurements from the same night have been averaged into a single data point. Error bars are omitted for clarity and are available with the full photometry in the electronic table.
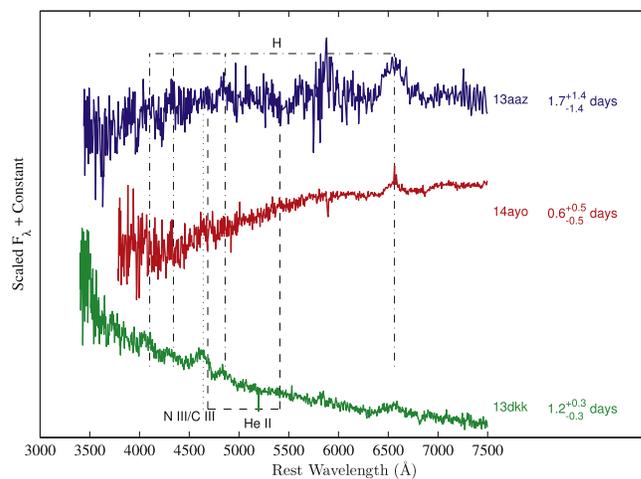
Figure 6. The first spectra of SNe that are <2 days old and were not classified as FI or BF. At right: the SN age, with respect to the estimated time of explosion (see the Appendix for details).

of the FI events have such a light curve. This suggests that either typical SN II-P progenitors have little CSM and do not produce FI features, or such features might be shorter lived for SNe II-P and have been missed in our data set. This is compatible with the finding that the spectrum of the SN II-P SN 2006bp, which is among the earliest yet obtained for objects of this class (Quimby et al. 2007; Gal-Yam et al. 2011), did show FI features and would have been picked up by our selection criteria (Table 2). Indeed, two of the SNe younger than 2 days
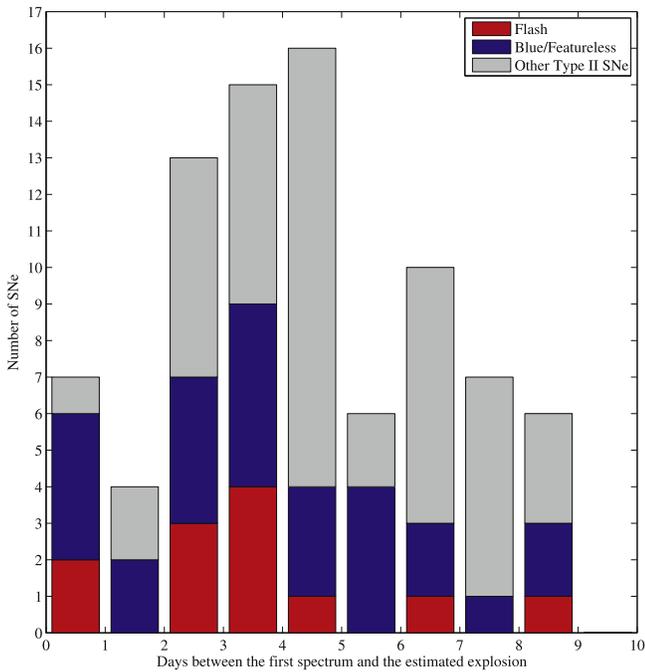
Figure 7. Number of SNe II with respect to the time between the first spectrum and the explosion. FI features appear even at relatively late phases, up to 9 days.

Table 3
Event Fractions

Days from Explosion	Sample Size	FI	BF
9	84	14%	32%
5	55	18%	33%
2	11	18%	54%
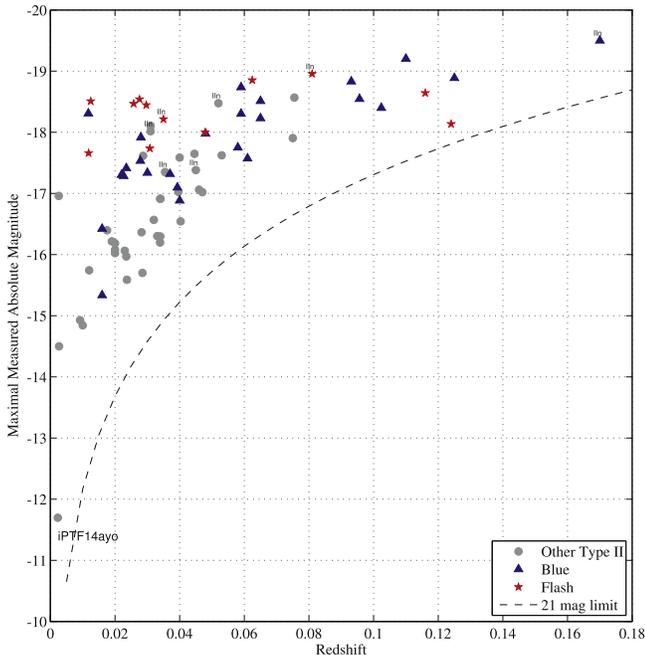
Figure 8. Maximal measured absolute magnitude in the R band (nine events with only early g-band photometry are omitted from this plot; two of these are BF) vs. the redshift. The dashed line corresponds to our average detection limit of $R = 21$ mag. iPTF14ayo is very faint, probably because of high extinction. FI and BF events dominate the high-luminosity end.

that are not FI or BF have light curves that are similar to those of faint SNe II-P and clearly differ from those of the FI events.

With early-time spectra that resemble those of iPTF13ast, the FI events show clear evidence for the existence of CSM around the progenitor. Assuming that this material was expanding at a velocity of $\sim$100 km s^{-1} (Groh 2014), and that the emission lines disappear after being swept away by the expanding ejecta moving typically at 10^4 km s^{-1}, and given that all of the FI events are constrained to be within 10 days after the explosion, we can conclude that such a CSM was ejected from the star $\sim$1000 days prior the explosion. SN spectra within 1 day after explosion may show additional emission lines (such as N IV; Gal-Yam et al. 2014) that disappear in only 1–2 days, so they are crucial in order to obtain the complete chemical composition of the CSM. Such early spectra also probe the nearby CSM, which was ejected from the progenitor just prior to the explosion. Subsequent early spectra would allow us to determine the temperature evolution of the SN. All of these reasons strongly motivate observing SNe as soon as possible after explosion.

5. SUMMARY

Motivated by the discovery of iPTF13ast showing prominent high-ionization emission lines in its early-time spectra, we searched the PTF and iPTF databases from 2009 until the end of 2014 for similar events. We found that FI signatures typically occur in SNe II, so we constructed a sample consisting of 84 SNe II whose first spectra are constrained to be within 10 days after explosion.

We classified the events in our sample according to their first spectra as FI, BF, or neither. We found that 14% of the SNe in our sample have FI signatures, whereas within 5 and 2 days after explosion the fraction is 18%. The actual fraction of FI events is likely higher, since FI SNe evolve into BF events as time progresses, and BF events develop normal SN features later on. Earlier spectra of a similar sample of events are expected to yield a higher fraction of FI events.

We obtained an interesting result regarding the connection between the SN temperature and its luminosity. In Figure 8 we see that at relatively high redshifts we have only BF and FI events. Those distant events are more luminous than average SNe II, as we expect from a flux-limited survey. However, we see in addition that 19 out of 21 events brighter than $M_R = -18.2$ mag are classified as BF or FI events. Since the lack of hydrogen lines in BF events and the existence of the He II emission line in FI events are an indication of high temperatures, and there are no interaction signatures >10 days after explosion, we conclude that more luminous SNe maintain higher temperatures during their early-time evolution.

Using flash spectroscopy, it should be possible to probe the material ejected from the progenitor $\sim$1000 days prior its explosion, reveal its elemental composition, track the SN early-time temperature evolution, and find the progenitor mass-loss rate shortly before the explosion. As our study shows, such events are not rare; thus, application of this method to future samples is a promising prospect.

APPENDIX
SAMPLE CONSTRUCTION

We started by looking for CC SNe that had a spectrum obtained within 6 days after PTF discovery[22] and found 332 events. All of the spectra were then classified as either BF events, FI events, or neither.

All 332 events were processed through our photometric pipeline in order to obtain a better estimate of the SN explosion time, and in many cases we found detections earlier than the PTF discovery.

In order to constrain the SN explosion date and the time of the pre-explosion limit, we did the following.

1. By default, we chose the date of the latest nondetection where the limiting magnitude (3 times the flux uncertainty, converted to magnitude) is fainter by at least 0.5 mag from the magnitude of the first detection. We then adopt an explosion date that is the mean date between the last nondetection and the first detection.

---

[22] Note that the discovery date can be a long time after the actual explosion.
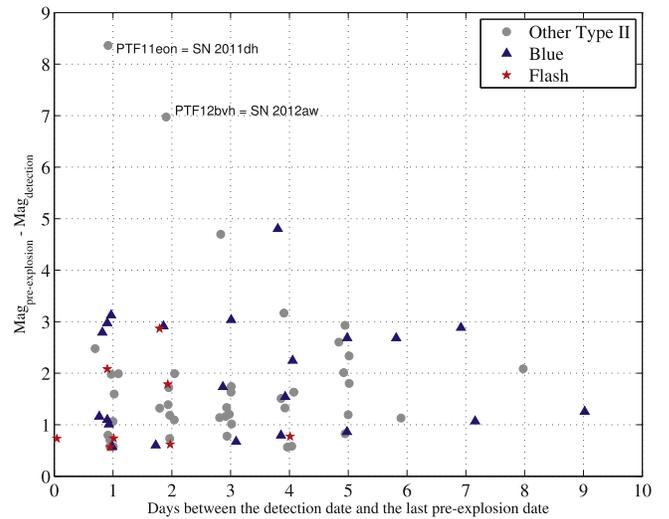
Figure 9. Magnitude difference between the pre-explosion limit and the first detection vs. the difference in days between the first detection and the pre-explosion (last nondetection) limit. All of the events with explosion time estimated by fitting the rise time (rather than using a recent pre-explosion limit) are omitted from this plot. SN 2011dh and SN 2012aw are nearby SNe with very deep nondetection limits, hence the large magnitude difference in a short time.

2. In the few cases where the spectrum was taken less than 10 days after the first detection, the pre-explosion limit was at least 1 day before the detection, and we had well-sampled photometry along the rise ($\geqslant 4$ nights of data before the peak). We calculated a parabolic fit to the data (all the data points along the rise) and chose the date when the flux was 0 as the explosion date. There were 19 such events in total; 3 of them are classified as FI and 5 as BF.

3. In the case of PTF10tel (SN 2010mc), which had a precursor (Ofek et al. 2013), we adopt as the SN explosion the mean between the date of the last precursor measurement and the date of the first measurement of the SN (main peak).

All 12 events showing FI signatures in their first spectrum were younger than 10 days from the time of the pre-explosion limit and are SNe II. We exclude a peculiar object of uncertain nature that possibly shows FI signatures and is the subject of a forthcoming publication (M. M. Kasliwal et al. 2016, in preparation). Hence, we omitted from further analysis all the events whose first spectra are not constrained to be within 10 days from explosion, and we focus on SNe II.

For one event we were unable to obtain reliable photometry in order to estimate its explosion time. This SN is at least 3 days old and is neither FI nor BF.

In order to check whether we missed any additional SNe having a spectrum obtained <10 days after explosion, we looked at all the CC SNe whose first spectrum was obtained within 10 days after PTF discovery. There are >100 additional events, but we found only five SNe II that match our selection criteria, and we added them to our sample.

We ended up with 84 SNe II in our sample, which includes all CC SNe whose first spectrum is constrained to have been obtained within 10 days after explosion.

Figure 9 shows the magnitude difference between the first detection magnitude and the limiting magnitude in the pre-
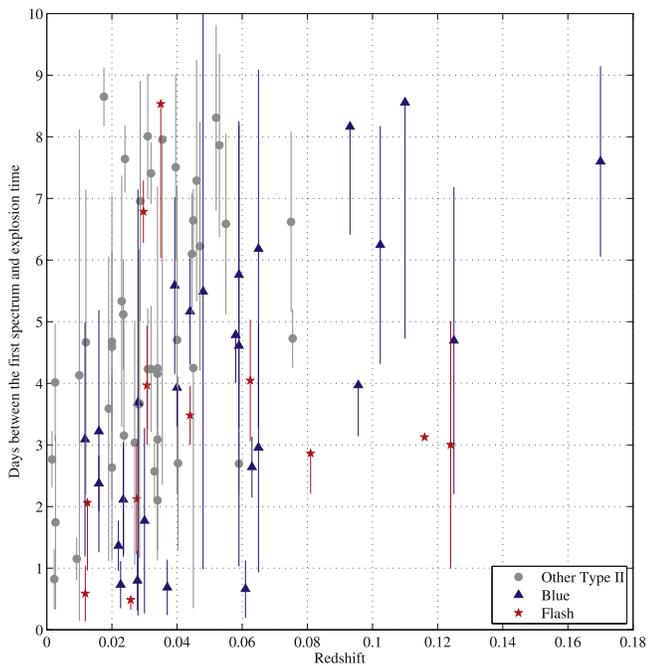
Figure 10. Time between the first spectrum and the estimated explosion time vs. the redshift. The error bars are between the times of the first detection and the pre-explosion limit (which is the same as the estimated explosion time for the SNe with fitted rise time). Note the lack of distant SNe that are not classified as BF or FI events.

explosion limit, versus the time difference between the two. In order to estimate an upper limit on the SN age, we required the limiting magnitude in the pre-explosion limit to be fainter by 0.5 mag with respect to the first detection. The resulting estimates are consistent with measurements based on well-sampled photometric light curves for all FI events (except PTF09ij, which does not have detailed photometry, and PTF10tel, which had a precursor). However, SNe may rise by ~3 mag within 10–20 days after the explosion, so our sample may have some contamination by old, slowly rising events that appear to be younger. This may be seen as the apparent excess of gray points around ~1 mag difference, compared to FI/BF events' domination at values of 2–3 mag. This contamination will result in estimating a lower fraction of FI events than the true one, making our reported fraction a lower limit.

For completeness, we present in Figure 10 the estimated age of SNe II in our sample versus their redshift. The error bars span the time between the first detection on the lower end and the pre-explosion limit on the other. Note that for some cases the time of the pre-explosion limit is the same as the estimated explosion time.

REFERENCES

Anderson, J. P., González-Gaitán, S., Hamuy, M., et al. 2014, ApJ, 786, 67
Arcavi, I., Gal-Yam, A., Cenko, S. B., et al. 2012, ApJL, 756, L30
Brink, H., Richards, J. W., Poznanski, D., et al. 2013, MNRAS, 435, 1047
Cardelli, J. A., Clayton, G. C., & Mathis, J. S. 1989, ApJ, 345, 245
Corsi, A., Ofek, E. O., Gal-Yam, A., et al. 2014, ApJ, 782, 42
Faran, T., Poznanski, D., Filippenko, A. V., et al. 2014, MNRAS, 445, 554
Filippenko, A. V. 1991, in SN 1987A and Other Supernovae, ed. I. J. Danziger, & K. Kjär (Garching: ESO), 343
Filippenko, A. V. 1997, ARA&A, 35, 309
Firth, R. E., Sullivan, M., Gal-Yam, A., et al. 2015, MNRAS, 446, 3895
Gal-Yam, A., Arcavi, I., Ofek, E. O., et al. 2014, Natur, 509, 471
Gal-Yam, A., Kasliwal, M. M., Arcavi, I., et al. 2011, ApJ, 736, 159
Garnavich, P. M., & Ann, H. B. 1994, AJ, 108, 1002
Graham, M. L., Sand, D. J., Valenti, S., et al. 2014, ApJ, 787, 163
Groh, J. H. 2014, A&A, 572, L11
Kiewe, M., Gal-Yam, A., Arcavi, I., et al. 2012, ApJ, 744, 10
Laher, R. R., Surace, J., Grillmair, C. J., et al. 2014, PASP, 126, 674
Langer, N. 2012, ARA&A, 50, 107
Law, N. M., Kulkarni, S. R., Dekany, R. G., et al. 2009, PASP, 121, 1395
Leonard, D. C., Filippenko, A. V., Barth, A. J., & Matheson, T. 2000, ApJ, 536, 239
Li, W., Leaman, J., Chornock, R., et al. 2011, MNRAS, 412, 1441
Margutti, R., Milisavljevic, D., Soderberg, A. M., et al. 2014, ApJ, 780, 21
Martin, J. C., Hambsch, F.-J., Margutti, R., et al. 2015, AJ, 149, 9
Matheson, T., Filippenko, A. V., Barth, A. J., et al. 2000, AJ, 120, 1487
Mauerhan, J. C., Smith, N., Filippenko, A. V., et al. 2013, MNRAS, 430, 1801
Niemela, V. S., Ruiz, M. T., & Phillips, M. M. 1985, ApJ, 289, 52
Ofek, E. O., Laher, R., Law, N., et al. 2012, PASP, 124, 62
Ofek, E. O., Sullivan, M., Cenko, S. B., et al. 2013, Natur, 494, 65
Ofek, E. O., Sullivan, M., Shaviv, N. J., et al. 2014, ApJ, 789, 104
Pastorello, A., Mattila, S., Zampieri, L., et al. 2008, MNRAS, 389, 113
Pastorello, A., Smartt, S. J., Mattila, S., et al. 2007, Natur, 447, 829
Phillips, M. M., Hamuy, M., Maza, J., et al. 1990, PASP, 102, 299
Quimby, R. M., Wheeler, J. C., Höflich, P., et al. 2007, ApJ, 666, 1093
Rahmer, G., Smith, R., Velur, V., et al. 2008, Proc. SPIE, 7014, 4
Rau, A., Kulkarni, S. R., Law, N. M., et al. 2009, PASP, 121, 1334
Rebbapragada, U., Bue, B., & Wozniak, P. R. 2015, in BAAS, 225, 43402
Sanders, N. E., Soderberg, A. M., Gezari, S., et al. 2015, ApJ, 799, 208
Schlegel, D. J., Finkbeiner, D. P., & Davis, M. 1998, ApJ, 500, 525
Schlegel, E. M. 1990, MNRAS, 244, 269
Shivvers, I., Groh, J. H., Mauerhan, J. C., et al. 2015, ApJ, 806, 213
Smartt, S. J., Eldridge, J. J., Crockett, R. M., & Maund, J. R. 2009, MNRAS, 395, 1409
Smith, N. 2014, ARA&A, 52, 487
Smith, N., Mauerhan, J. C., Cenko, S. B., et al. 2015, MNRAS, 449, 1876
Taddia, F., Stritzinger, M. D., Sollerman, J., et al. 2013, A&A, 555, A10
Wozniak, P. R., Moody, D. I., Ji, Z., et al. 2013, in BAAS, 221, 43105
Yaron, O., & Gal-Yam, A. 2012, PASP, 124, 668
Zhang, J., Wang, X., Mazzali, P. A., et al. 2014, ApJ, 797, 5